Inorg. Chem. **2003**, *42*, 6898–6906

4,4′-Dithiodipyridine as a Bridging Ligand in Osmium and Ruthenium Complexes: The Electron Conductor Ability of the –S–S– Bridge#

Welter C. Silva,[†,‡] Joacy B. Lima,[†] Icaro S. Moreira,[‡] Antônio M. Neto,[§] Flávio C. G. Gandra,[§] Antônio G. Ferreira,[||] Bruce R. McGarvey,[⊥] and Douglas W. Franco*,[†]

Instituto de Química de São Carlos, Departamento de Química e Física Molecular, Universidade de São Paulo, Cx. Postal 780, CEP. 13560-970, São Carlos-SP, Brazil, Departamento de Química Orgânica e Inorgânica, Universidade Federal do Ceará, Cx. Postal 6032, CEP. 60455-900, Fortaleza-CE, Brazil, Departamento de Física, Universidade Estadual de Campinas, Campinas-SP, Brazil, Departamento de Química, Universidade Federal de São Carlos, São Carlos-SP, Brazil, and Department of Chemistry and Biochemistry, University of Windsor, Windsor, Ontario, Canada N9B 3P

Received June 6, 2003

The compounds $[Ru(NH_3)_5(dtdp)](TFMS)_3$, $[Os(NH_3)_5(dtdp)](TFMS)_3$, $[(NH_3)_5Os(dtdp)Os(NH_3)_5](TFMS)_6$, $[(NH_3)_5Os(dtdp)Ru(NH_3)_5](TFMS)_3(PF_6)_2$, and $[(NH_3)_5Os(dtdp)Fe(CN)_5]$ (dtdp = 4,4′-dithiodipyridine, TFMS = trifluoromethanesulfonate) have been synthesized and characterized by elemental analysis, cyclic voltammetry, electronic, vibrational, EPR, and ^1H NMR spectroscopies. Changes in the electronic and voltammetric spectra of the ion complex $[Os(NH_3)_5(dtdp)]^{3+}$ as a function of the solution pH enable us to calculate the pK_a for the $[Os(NH_3)_5(dtdpH)]^{4+}$ and $[Os(NH_3)_5(dtdpH)]^{3+}$ acids as 3.5 and 5.5, respectively. The comparison of the above pK_a data with that for the free ligand (pK_1 = 4.8) provides evidence for the –S–S– bridge efficiency as an electron conductor between the two pyridine rings. The symmetric complex, $[(NH_3)_5Os(dtdp)Os(NH_3)_5]^{6+}$, is found to exist in two geometric forms, and the most abundant form (most probably trans) has a strong conductivity through the –S–S– bridge, as is shown by EPR, which finds it to have an $S = 1$ spin state with a spin–spin interaction parameter of 150–200 G both in the solid sate and in frozen solution. Further the NMR of the same complex shows a large displacement of unpaired spin into the π orbitals of the dttp ligand relative to that found in $[Os(NH_3)_5(dtdp)]^{3+}$. The comproportionation constant, $K_c = 2.0 \times 10^5$, for the equilibrium equation $[Os^{II}Os^{II}] + [Os^{III}Os^{III}] \rightleftharpoons 2[Os^{II}Os^{III}]$ and the near-infrared band energy for the mixed-valence species (MMCT), $[(NH_3)_5Os(dtdp)Os(NH_3)_5]^{5+}$ (λ_{MMCT} = 1665 nm, $\epsilon = 3.5 \times 10^3$ M^{-1} cm^{-1}, $\Delta\bar{\nu}_{1/2} = 3.7 \times 10^3$ cm^{-1}, $\alpha = 0.13$, and $H_{AB} = 7.8 \times 10^2$ cm^{-1}), are quite indicative of strong electron delocalization between the two osmium centers. The electrochemical and spectroscopic data for the unsymmetrical binuclear complexes $[(NH_3)_5Os^{III}(dtdp)Ru^{II}(NH_3)_5]^{5+}$ (λ_{MMCT} = 965 nm, $\epsilon = 2.2 \times 10^2$ M^{-1} cm^{-1}, $\Delta\bar{\nu}_{1/2} = 3.0 \times 10^3$ cm^{-1}, and $H_{AB} = 2.2 \times 10^2$ cm^{-1}) and $[(NH_3)_5Os^{III}(dtdp)Fe^{II}(CN)_5]$ (λ_{MMCT} = 790 nm, $\epsilon = 7.5 \times 10$ M^{-1} cm^{-1}, $\Delta\bar{\nu}_{1/2} = 5.4 \times 10^3$ cm^{-1}, and $H_{AB} = 2.0 \times 10^2$ cm^{-1}) also suggest a considerable electron delocalization through the S–S bridge. As indicated by a comparison of K_c and energy of the MMCT process in the iron, ruthenium, and osmium complexes, the electron delocalization between the two metal centers increases in the following order: Fe < Ru < Os.

Introduction

Electron-transfer reactions play central roles in physical, chemical, and biological processes. One of central themes of bioinorganic research has been the elucidation of the factors that determine electron-transfer rates in metalloproteins.[1,2] Inorganic complexes containing metal centers with valence electrons in *n*d orbitals of different radial extensions, oxidation states, and coordination spheres can provide access

* Corresponding author. Fax: +55-16-273-9976. E-mail: douglas@iqsc.usp.br.

This paper is dedicated in memoriam to our master and friend Geraldo Vicentini.

† Universidade de São Paulo.
‡ Universidade Federal do Ceará.
§ Universidade Estadual de Campinas.
|| Universidade Federal de São Carlos.
⊥ University of Windsor.

(1) Johnson, M. K.; King, R. B.; Kurtz, D. M., Jr.; Kutal, C.; Norton, M. L.; Scott, R. A. *Electron Transfer in Biology in the Solid State Inorganic Compounds with Unusual Properties*; American Chemical Society, Washington, 1990.
(2) Zuckerman, J. J. *Electron Transfer and Electrochemical Reactions; Photochemical and Other Energized Reactions in Inorganic Reactions and Methods, Vol.15*; VCH Publishers: Deerfield Beach, FL, 1986.
(3) Isied, S. S. *Metal Ions in Biological Systems*; Sigel H., Ed.; Dekker: New York, 1991; pp 1−56.

10.1021/ic034630o CCC: $25.00
Published on Web 09/18/2003

to useful new information to understanding these processes in biological[3] and in superconductor systems.[4]

Iron, ruthenium, and osmium complexes in d^5 and d^6 low-spin electronic configurations are well-known to be inert regarding substitution reactions and to exhibit high affinity for N-heterocycle ligands.[5−15] These metal centers in the above electronic configurations have orbitals of proper symmetry and energy to interact with relatively low energy, unoccupied π^* orbitals in the pyridine ligands. These M(II)−py or M(III)−py bonds are thermodynamically very stable and kinetically inert.[13−15]

As a consequence of the 5d orbitals' large radial extension, the osmium metal centers in II and III oxidation states, when coordinated to the N-heterocyclic ligands, are expected to produce highly stable complexes due to the Os→N-heterocyclic back-bonding interaction.[8,16]

We have accumulated evidence on mono- and binuclear, homo- and heteronuclear complexes, of iron and ruthenium which show the capacity of the −S−S− bridge to act as an electron conductor.[5,6] An extensive comparison has been carried out on other systems available in the literature[5,6] which shows the higher efficiency of the −S−S− bridge over the majority of the other bridges and strongly suggests that the coupling occurs through the −S−S− group and not by a through-space interaction between the two metal centers. Indeed, data for similar systems Mpy−(CH_2CH_2)−pyM[7b−d] available in the literature clearly shows the absence of coupling between the metal centers. Furthermore, in binuclear ruthenium complexes using py−(CH_2−S−S−CH_2)−py and py−(S)−py as bridging ligands[5,6] only very weak coupling has been observed pointing out the relevance of the −S−S− fragment.

As a part of our efforts to understand the role of the −S−S− bridge on electron conduction, this work reports experiments using Os(II), Os(III), and Ru(III) metal centers as probes.

Experimental Section

Chemicals and Reagents. The solvents ethanol, acetone, ethyl ether, and dichloromethane were purified according to standard procedures,[17] and double-distilled water was used throughout. All the other chemical reagents were of analytical grade purity.

Synthesis. The compounds $[Os(NH_3)_5(TFMS)](TFMS)_2$,[18] $[Os(NH_3)_5(H_2O)](TFMS)_3$,[19] $[Ru(NH_3)_5(H_2O)](TFMS)_3$,[20] $[Ru(NH_3)_5(H_2O)](PF_6)_2$,[21] and $Na_3[Fe(CN)_5(NH_3)]\cdot 3H_2O$[22] were prepared by literature methods and their characteristics checked by UV−visible and IR spectroscopy and electrochemical techniques.

$[Os(NH_3)_5(dtdp)](TFMS)_3$. $[Os(NH_3)_5(H_2O)](TFMS)_3$ complex (100 mg, 0.14 mmol) was added to a solution of dtdp ligand (300 mg, 1.36 mmol) in 10 mL of deaerated acetone. The mixture was kept at 25 °C and stirred for 5 h, under argon flow. The $[Os(NH_3)_5(dtdp)](TFMS)_3$ complex was precipitated by adding 40 mL of dichloromethane, and the solid was filtered under argon, washed with deaerated dichloromethane, and dried in a vacuum. Yield: 90%. Anal. Calcd: C, 16.7; H, 2.46; N, 10.4. Found: C, 16.5; H, 2.52; N, 10.3.

$[Ru(NH_3)_5(dtdp)](TFMS)_3\cdot 4H_2O$. $[Ru(NH_3)_5(H_2O)](TFMS)_3$ complex (100 mg, 0.15 mmol) was added to a solution of dtdp ligand (300 mg, 1.36 mmol) in 10 mL of deaerated acetone. The mixture was kept at 25 °C and stirred for 24 h, under argon flow. The $[Ru(NH_3)_5(dtdp)](TFMS)_3\cdot 4H_2O$ complex was precipitated by adding 40 mL of dichloromethane, and the solid was filtered under argon, washed with deaerated dichloromethane, and dried in a vacuum. Yield: 70%. Anal. Calcd: C, 16.3; H, 3.37; N, 10.6. Found: C, 16.0; H, 3.31; N, 10.6.

$[(NH_3)_5Os(dtdp)Os(NH_3)_5](TFMS)_6$. The $[(NH_3)_5Os(dtdp)Os(NH_3)_5](TFMS)_6$ complex was synthesized by reacting $[Os(NH_3)_5(dtdp)](TFMS)_3$ and $[Os(NH_3)_5(TFMS)](TFMS)_2$ in a 1:1 stoichiometric ratio. In a reaction flask, 65.5 mg (0.069 mmol) of $[Os(NH_3)_5(dtdp)](TFMS)_3$ complex was dissolved in 0.30 mL of deaerated acetone. $[Os(NH_3)_5(TFMS)](TFMS)_2$ complex (50.2 mg, 0.069 mmol) was dissolved in 0.20 mL of deaerated acetone and added to the solution that contained the mononuclear complex. This solution of dark brown color was stirred while kept under an argon stream for 5 h. Adding 20 mL of dichloromethane precipitated the binuclear symmetric complex, and the solid obtained was collected in a sintered glassy filter and washed with dichloromethane. The desired complex was purified by cation-exchange chromatography from SP-Sephadex C 25 in the same way as described for other osmium compounds.[7a] The fraction eluted with 1.0−1.5 HTFMS was collected and rotary-evaporated to dryness. The pure dimer compound was obtained by dissolving the solid in 2.0 mL of acetone and then precipitated with addition of 30 mL of dichloromethane. The binuclear complex solid obtained was collected in a sintered glassy, stored in a desiccator, under vacuum, and in the absence of light. Yield: 65%. Anal. Calcd: C, 11.5; H, 2.30; N, 10.1. Found: C, 11.4; H, 2.23; N, 10.0.

$[(NH_3)_5Os(dtdp)Ru(NH_3)_5](TFMS)_3(PF_6)_2$. The $[(NH_3)_5Os^{(III)}(dtdp)Ru^{(II)}(NH_3)_5](TFMS)_3(PF_6)_2$ complex was synthesized by reacting $[Os(NH_3)_5(dtdp)](TFMS)_3$ and $[Ru(NH_3)_5(H_2O)](PF_6)_2$ in a 1:1 stoichiometric ratio. In a reaction flask, 94.3 mg (0.1 mmol) of $[Os(NH_3)_5(dtdp)](TFMS)_3$ complex was dissolved in 10 mL of deaerated acetone. 49.4 mg (0.1 mmol) of $[Ru(NH_3)_5(H_2O)](PF_6)_2$

(4) Lewis, N. A.; Obeng, S. Y.; Taveras, D. V.; van Eldik, R. J. *J. Am. Chem. Soc.* **1989**, *111*, 924−927.
(5) (a) Moreira, I. S.; Franco, D. W. *Inorg. Chem.* **1994**, *35*, 1607−1613. (b) Moreira, I. S.; Franco, D. W. *Adv. Chem. Ser.* **1997**, *253*, 254−266.
(6) Moreira, I. S.; Lima, J. B.; Franco, D. W. *Coord. Chem. Rev.* **2000**, *196*, 197−217.
(7) (a) Lay, P. A.; Magnuson, R. H.; Taube, H. *Inorg. Chem.* **1988**, *27*, 2848−2853. (b) Powers, M. J.; Meyer, T. J. *J. Am. Chem. Soc.* **1980**, *102*, 1289−1297. (c) Callahan, R. W.; Brown, G. M.; Meyer, T. J. *Inorg. Chem.* **1975**, *14*, 1443−1453. (d) Olabe, J. A.; Haim, A. *Inorg. Chem.* **1989**, *28*, 3277−3278.
(8) Sen, J.; Taube, H. *Acta Chem. Scand.* **1979**, *A33*, 125−135.
(9) Lay, P. A.; Magnuson, R. H.; Taube, H. *Inorg. Chem.* **1989**, *28*, 3001−3007.
(10) Creutz, C.; Chou, M. H. *Inorg. Chem.* **1987**, *26*, 2995−3000.
(11) Matsubara, T.; Ford, P. C. *Inorg. Chem.* **1976**, *15*, 1107−1110.
(12) Allen, R. J.; Ford, P. C. *Inorg. Chem.* **1973**, *11*, 679−685.
(13) Ford, P. C. *Coord. Chem. Rev.* **1970**, *5*, 75.
(14) Shepherd, R. E.; Taube, H. *Inorg. Chem.* **1973**, *12*, 1392−1401.
(15) Johnson, C. R.; Shepherd, R. E. *Inorg. Chem.* **1983**, *22*, 1117−1123.
(16) Sekine, M.; Harman, W. D.; Taube, H. *Inorg. Chem.* **1988**, *27*, 3604−3608.
(17) Perrin, D. D.; Armarego, W. L. F.; Perrin, D. R. *Purification of Laboratory Chemicals*, 2nd ed.; Pergamon Press: New York, 1980.
(18) Lay, P. A.; Magnuson, R. H.; Sen, J.; Taube, H. *J. Am. Chem. Soc.* **1982**, *104*, 7658−7659.
(19) Lay, P. A.; Magnuson, R. H.; Taube, H. *Inorg. Synth.* **1986**, *24*, 271−273.
(20) Kreuztian, H. *Mixed Valence Ruthenium Ammine Dinitrile and Related Complexes*, Ph.D. Thesis, Stanford University, 1976.
(21) Kuehn, C. G.; Taube, H. *J. Am. Chem. Soc.* **1976**, *98*, 689−702.
(22) Brauer, G. *Handbook of Preparative Inorganc Chemistry*; Academic Press: New York, 1965.

complex was added to this solution, and the reaction mixture was stirred while kept under an argon stream for 2 h. The solution was transferred to a 50 mL round-bottom flask, and the solvent was evaporated to half of its initial volume. To the resulting solution was added 30 mL of deaerated dichloromethane. The brown product, unsymmetrical binuclear complex, was quickly precipitated. The solid obtained was collected in a sintered glassy filter, washed with dichloromethane, and stored in a desiccator, under vacuum, in the absence of light. Yield: 90%. Anal. Calcd: C, 11.0; H, 2.70; N, 11.8. Found: C, 11.3; H, 2.77; N, 11.4.

$[(NH_3)_5Os(dtdp)Fe(CN)_5]$. The $[(NH_3)_5Os(dtdp)Fe(CN)_5]$ complex was synthesized by reacting $[Os(NH_3)_5(dtdp)](TFMS)_3$ and $Na_3[Fe(CN)_5(NH_3)]\cdot 3H_2O$ in a 1:1 stoichiometric ratio: 51.4 mg (0.054 mmol) of $[Os(NH_3)_5(dtdp)](TFMS)_3$ was dissolved in 0.5 mL of deaerated acetone, and 17.6 mg (0.054 mmol) of $Na_3[Fe(CN)_5(NH_3)]\cdot 3H_2O$ complex were dissolved in 0.5 mL of acetone/water (80%) and added to the solution that contained the mononuclear complex of osmium(III). Immediately the formation of a dark green product occurred. The resulting solution was stirred, while kept under an argon stream, for 1 h. This unsymmetrical binuclear complex was collected in a sintered glassy filter, washed with dichloromethane, and stored in a desiccator, under vacuum, in the absence of light. Yield: 75%. Anal. Calcd: C, 26.4; H, 3.40; N, 24.6. Found: C, 26.3; H, 3.34; N, 24.4.

Apparatus, Techniques, and Calculation Methods. The manipulations were carried out in the absence of oxygen, under nitrogen or argon atmosphere following standard procedures.[23] All the complexes were stored under vacuum and protected from light. Ultraviolet and visible spectra were recorded on a Hewlett-Packard 8452A spectrophotometer. The near-infrared spectra were recorded on a HITACHI U3501, in D_2O, at 25 °C. The [II,III] mixed-valence species have been generated in D_2O solutions (0.01 M DCl) by reduction with Eu(II) of the corresponding fully oxidized [III,III] symmetric binuclear complex of osmium. The ^1H NMR spectra were recorded on a Bruker AC-200 and ARX-400 spectrometers, respectively. The NMR spectra were performed in acetone-d_6 solutions, using tetramethylsilane (TMS) as internal standard. In some cases the NMR assignments for the ligand dttp have been checked by decoupling experiments. We used for EPR experiments a Bruker ESP300e spectrometer operating with an X-band microwave bridge. The measurements were carried out at liquid nitrogen temperature. The EPR simulations were done with a program written by one of the authors. The electrochemical measurements were performed using a PARC system model 173 potentiostat/galvanostat, a model 175 universal programmer, and a RE 0074X-Y recorder and a model 264A polarographic analyzer. A glassy carbon electrode was used as working electrode, SCE as reference, and a platinum wire as auxiliary electrode.[24]

Results and Discussion

Electronic Spectra. The spectral characteristics of the $[Os(NH_3)_5(dtdp)]^{3+}$, $[Os(NH_3)_5(dtdpH)]^{4+}$, $[Os(NH_3)_5(dtdp)]^{2+}$, $[Os(NH_3)_5(dtdpH)]^{3+}$, $[Ru(NH_3)_5(dtdp)]^{3+}$, and $[Ru(NH_3)_5(dtdpH)]^{4+}$ complexes and the band assignments are summarized in Table 1.

The electronic spectrum of the $[Os(NH_3)_5(dtdp)]^{3+}$ species exhibits strong absorptions at 228 ($\epsilon = 3.6 \times 10^3$ M^{-1} cm^{-1}) and 252 nm ($\epsilon = 8.7 \times 10^3$ M^{-1} cm^{-1}) assigned to internal ligand transitions (IL) and at 312 nm ($\epsilon = 1.1 \times 10^4$ M^{-1} cm^{-1}) attributed to metal-to-ligand charge transfer (MLCT). A more careful analysis using Gaussian deconvolution[25] allowed us to detect one additional band at 387 nm ($\epsilon = 5.0 \times 10^2$ M^{-1} cm^{-1}), which could be, at the first sight, assigned to be ligand field (LF) in character, due to its low molar absorptivity. However, a charge-transfer character has been attributed[7,8] to a similar low-energy band in osmium pentaammine complexes with N-heterocycle ligands. Alternatively this absorption (387 nm) has been interpreted as consequence of the MLCT band (312 nm) splitting due to the spin−orbit coupling.[7,8] This last interpretation can be rejected on the basis of our analysis of the EPR results which predict a much smaller splitting.

Table 1. Absorption Data of Mononuclear Complexes of Osmium and Ruthenium with dtdp Ligand

species	attributions: IL (λ, nm) ($\epsilon \times 10^{-4}$, M^{-1} cm^{-1})	MLCT (λ, nm) ($\epsilon \times 10^{-4}$, M^{-1} cm^{-1})	LMCT (λ, nm) ($\epsilon \times 10^{-4}$, M^{-1} cm^{-1})	d−d (λ, nm) ($\epsilon \times 10^{-3}$, M^{-1} cm^{-1})
dtdp[a]	230 (1.10)			
	256 (1.50)			
	290 (1.00)			
$(dtdpH)^{+}$ [a]	230 (1.10)			
	294 (1.45)			
$(dtdpH_2)^{2+}$ [a]	236 (0.93)			
	274 (1.42)			
	320(1.45)			
$[Os(NH_3)_5(dtdp)]^{3+}$	228 (0.36)	312 (1.10)		387 (0.50)
	252 (0.87)			
$[Os(NH_3)_5(dtdp)]^{2+}$	225 (1.10)	470 (0.75)		
	248 (1.80)			
$[Os(NH_3)_5(dtdpH)]^{4+}$	230 (0.90)	328 (1.40)		
	274 (1.10)			
$[Os(NH_3)_5(dtdpH)]^{3+}$	224 (1.00)	488 (0.85)		
	255 (0.68)			
	291 (1.20)			
$[Ru(NH_3)_5(dtdp)]^{3+}$	213 (0.51)		280 (0.66)	420 (1.00)
	248 (0.85)			
$[Ru(NH_3)_5(dtdpH)]^{4+}$	217 (1.40)		281 (1.70)	
	249 (0.96)			
$[Ru(NH_3)_5(dtdp)]^{2+}$ [b]	256 (1.50)	458 (1.30)		
	286 (1.00)			
$[Ru(NH_3)_5(dtdpH)]^{3+}$ [b]	260 (1.10)	474 (1.40)		
	292 (1.20)			

[a] Reference 26. [b] Reference 5.

The $[Os(NH_3)_5(dtdpH)]^{4+}$ ion was generated in aqueous solution (HTFMS, 0.1 M, pH 1.5) by protonation of the pyridine ring. The protonation effects on the spectrum can be observed as bathochromic shifts in the MLCT and intraligand (IL) bands. The spectrum of the protonated species exhibits an MLCT band at 328 nm ($\epsilon = 1.4 \times 10^4$ M^{-1} cm^{-1}) in addition to the IL bands at 230 nm ($\epsilon = 9.0 \times 10^3$ M^{-1} cm^{-1}) and 274 nm ($\epsilon = 1.1 \times 10^4$ M^{-1} cm^{-1}). These IL bands exhibit bathochromic shifts very similar to those observed in the free ligand (see Table 1). The difference in energy of the MLCT band for $[Os(NH_3)_5(dtdp)]^{3+}$ and $[Os(NH_3)_5(dtdpH)]^{4+}$ species ($\Delta\bar{\nu} = 1564$ cm^{-1}), when compared to the similar ruthenium and iron complexes,[5,6] suggests a stronger back-bonding interaction in the Os center.

The reduction of the $[Os(NH_3)_5(dtdp)]^{3+}$ ion with Zn(Hg) in aqueous media produced a green species, corresponding

(23) Shriver, D. F. The Manipulation of Air-Sensitive Compounds; McGraw-Hill Co.: New York, 1969.
(24) Meites, L. *Polarographic Techniques*, 2nd ed.; Interscience: New York, 1965; Chapter 5.
(25) *Microcal Origin*, version 5.0; Microcal Software: Northampton, MA, 1997.

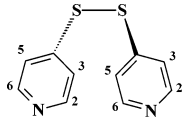

Figure 1. 4,4′-Dithiodipyridine (dtdp).

to the Os(II) complex. This reduced species shows an MLCT absorption at 470 nm, which is bathochromic shifted ($\Delta\bar{\nu} = 10775\ cm^{-1}$) relative to the MLCT band of the $[Os(NH_3)_5(dtdp)]^{3+}$ (312 nm). This behavior is similar to that observed for analogous ruthenium species.[5,6]

The $[Os(NH_3)_5(dtdpH)]^{3+}$ species was generated in aqueous solution (CF_3COOH, 0.1 M) by reducing the corresponding Os(III) species with Zn(Hg). The spectrum of this complex exhibits MLCT absorption at 488 nm ($\epsilon = 8.5 \times 10^3\ M^{-1}\ cm^{-1}$) and IL bands at 224 nm ($\epsilon = 1.0 \times 10^4\ M^{-1}\ cm^{-1}$), 255 nm ($\epsilon = 0.68 \times 10^4\ M^{-1}\ cm^{-1}$), and 291 nm ($\epsilon = 1.2 \times 10^4\ M^{-1}\ cm^{-1}$). The MLCT band (488 nm) is at a lower energy than the MLCT band (470 nm) of the $[Os(NH_3)_5(dtdp)]^{2+}$ species. This was expected since the protonation of the uncoordinated pyridine ring stabilizes the orbital π^* of the ligand facilitating the back-bonding interaction.[13,15]

As observed (see Table 1), the (MLCT) absorption for the $[Os(NH_3)_5(dtdp)]^{3+}$ and $[Os(NH_3)_5(dtdp)]^{2+}$ species occurs at lower energy than those of the corresponding py complex.[8] These observations are consistent with the π^* orbital in dtdp being lower in energy than the π^* orbital in the pyridine ligand.[8]

Besides the IL bands at 213 ($\epsilon = 5.1 \times 10^3\ M^{-1}\ cm^{-1}$) and 248 nm ($\epsilon = 8.5 \times 10^3\ M^{-1}\ cm^{-1}$), the $[Ru(NH_3)_5(dtdp)]^{3+}$ ion exhibits a band centered at 280 nm ($\epsilon = 6.6 \times 10^3\ M^{-1}\ cm^{-1}$), tentatively attributed as LMCT, and a transition at 420 nm ($\epsilon = 1.0 \times 10^3\ M^{-1}\ cm^{-1}$), probably LF in character. The ligand protonation in $[Ru(NH_3)_5(dtdpH)]^{4+}$ does not lead to any change in the spectrum.

NMR. The ^1H NMR spectrum of dtdp ligand (see Figure 1) in acetone-d_6 contains two signals with double peaks centered in δ 8.52 ($J = 4.6$; 1.6 Hz) assigned to protons 2,6 and δ 7.51 ($J = 4.6$; 1.6 Hz) assigned to protons 3,5, based on an A_2X_2 reference system.[5,6,27,28]

The chemical shifts for the diamagnetic $[Ru(NH_3)_5(dtdp)](PF_6)_2$ are δ 8.52 ($J = 4.5$; 1.6 Hz), 7.34 ($J = 4.5$; 1.6 Hz) for hydrogens 2,6 and 3,5 in the uncoordinated pyridine ring, δ 8.80 ($J = 5.3$; 1.6 Hz), 7.28 ($J = 5.3$; 1.6 Hz) for hydrogens 2,6 and 3,5 in the coordinated pyridine ring, and two broad signals at δ 2.91 and 2.57 for NH_3 groups. These were used as reference signals in calculating the paramagnetic shifts above for $[Os(NH_3)_5(dtdp)](TFMS)_3$.

For the $[Os(NH_3)_5(dtdp)](TFMS)_3$, we found four signals in the NMR spectrum centered in δ 8.52 ($J = 5.5$ Hz), 8.17 ($J = 5.5$ Hz), 7.54 d ($J = 5.5$ Hz), and 6.71 ($J = 5.5$ Hz), and two broad signals at δ 150.1 and 88.1 which correspond to the equatorial and axial NH_3 groups, respectively, that

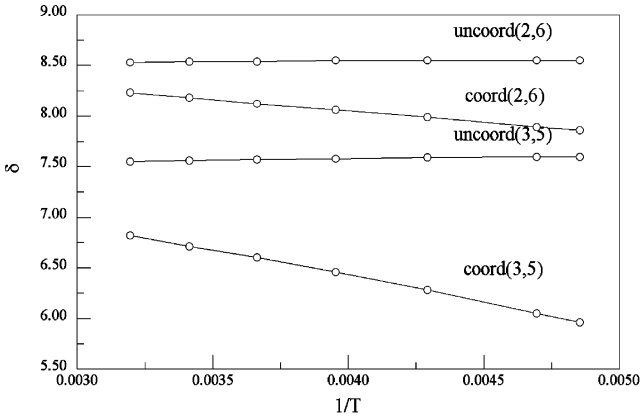

Figure 2. ^1H NMR of dtdp in $[Os(NH_3)_5(dtdp)](TFMS)_3$ in *d*-acetone as a function of the inverse temperature.

disappeared when drops of D_2O were added into the solution. The signals at δ 8.52 and 7.54 were assigned to the hydrogens 2,6 and 3,5 respectively of the uncoordinated pyridine ring, and the signals at δ 8.17 and 6.71 correspond to the hydrogens 2,6 and 3,5 of the coordinated pyridine ring. The assignments for the hydrogens on the coordinated ring and the paramagnetic origin for their shifts were confirmed by the temperature dependence observed for the lines shown in Figure 2. The chemical shifts, in the deshielding spectrum region, for the NH_3 groups are due to the large paramagnetic shift arising from the adjacent Os^{3+}. They are to be compared to the shifts observed[29] in $[Os(NH_3)_5(H_2O)]^{3+}$ at 125 and 110 ppm and in $[Ru(NH_3)_5(H_2O)]^{3+}$ at 147.6 and 124.2 ppm, except that in this complex the larger shifts are associated with the axial ammonia hydrogens. The large line widths of the NH_3 signals are due partly to ^{14}N quadrupolar effects and to short T_1's resulting from strong magnetic dipolar interactions with the magnetic metal ion.

The origin and theory of the paramagnetic shift for the NH_3 hydrogens areis treated in detail in an earlier paper.[29] The paramagnetic shifts for the 2,6 and 3,5 hydrogens in the coordinated ring are $(8.17-8.80) = -0.63$ and $(6.71-7.28) = -0.57$, respectively. Using the g values, discussed below, for the ground state of Os^{3+} we can estimate[29] the pseudocontact shift for these hydrogens as 6.35 and -1.44. This gives for the contact shift values of -6.98 and 0.87 ppm, indicating considerable spin density at the 2,6 site and very little at the 3,5 site. There is a slight temperature shift observed for the 3,5 site on the uncoordinated ring, probably from the pseudocontact shift.

Similar behavior was observed in the $[Ru(NH_3)_5(dtdp)](TFMS)_3$ spectrum. Six signals can be identified: δ 8.63 ($J = 5.4$ Hz), 7.76 ($J = 5.4$ Hz) corresponding to hydrogens 2,6 and 3,5 in the uncoordinated pyridine ring, two multiplets centered in δ 8.13 and δ 6.66 corresponding to hydrogens in the coordinated pyridine ring, and two broad NH_3 signals at δ 185.3 and 104.2. These chemical shifts are very similar to those observed for the osmium compound.

The NMR of $[(NH_3)_5Os(dtdp)Os(NH_3)_5](TFMS)_6$, as well as the EPR to be discussed below, presented problems of

(26) Moreira, I. S.; Parente, L. T. S.; Franco, D. W. *Quím. Nova* **1998**, *21* (5), 545−550.
(27) Forchioni, A.; Pappalardo, G. *Spectrochim. Acta* **1975**, *31-A*, 1367.
(28) Moreira, I. S.; Franco, D. W. *J. Chem. Soc., Chem. Commun.* **1992**, *5*, 450−451.
(29) McGarvey, B. R.; Batista, N. C.; Bezerra, W. B.; Schultz, M. S.; Franco, D. W. *Inorg. Chem.* **1998**, *37*, 2865−2872.

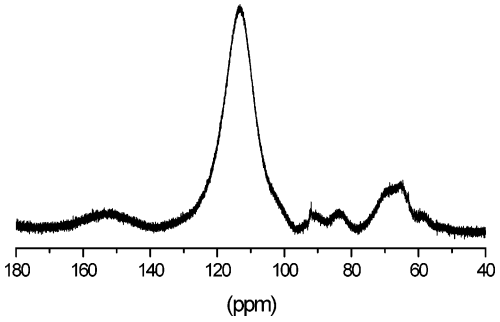

Figure 3. ^{1}H NMR of the ion complex $[(NH_3)_5Os(dtdp)Os(NH_3)_5]^{6+}$ in *d*-acetone in downfield region. The spectrum is from the sample purified by cation-exchange chromatography.

inconsistency until great care was taken to exclude water and oxygen from the solution, because the spectra changed with time, suggesting that some reaction was taking place. Even so, the NMR spectrum showed the existence of at least three paramagnetic species in solution at room temperature, as can be seen in Figure 3, which shows six ammonia proton peaks (151, 113, 90, 84, 67, and 59 ppm) from the $Os^{III}(NH_3)_5$ component of the binuclear complex. A single $Os^{III}(NH_3)_5$ should give two peaks for the equatorial and axial ammonias in the ratio of 4:1. At first we suspected that we had decomposition into starting reagents since the peaks at 151 ppm and at 90 ppm are close to the peaks of $[Os(NH_3)_5(dtdp)](TFMS)_3$ mentioned above and the peak at 67 ppm could be identified as the axial peak for $[Os(NH_3)_5(TFMS)](TFMS)_2$, whose equatorial peak is found at 114 ppm. However, repeated preparations plus purification using column ion cation-exchange chromatography (Sephadex C25) produce similar NMR spectra differing slightly in the relative intensities among the weaker peaks. Cyclic voltammetry and UV−visible data show that any decomposition in the first 24 h is less than 5%. Therefore it seems likely that all of these peaks must be different forms of $[(NH_3)_5Os(dtdp)Os(NH_3)_5](TFMS)_6$. From intensity, we can identify the peak at 113 ppm as the equatorial ammonia peak of the main form with the peak at 64 ppm being the axial ammonia. These two peaks make up 85−90% of all the ammonia peaks observed. This is the form that is identified below by EPR to be a triplet state molecule with $S = 1$. For reasons that will be discussed below we believe the two peaks at 151 and 90 ppm to be the equatorial and axial ammonias of a biradical ($S = {}^1/_2$) form of $[(NH_3)_5Os(dtdp)Os(NH_3)_5](TFMS)_6$. The weakest peaks at 84 and 59 ppm are unassigned.

Analysis of the ligand protons has its problems also. The largest peaks at 2.0 and 5.8 ppm are due to *d*-acetone and dichloromethane, respectively. There are many small peaks between 6 and 11 ppm; four of them are ligand peaks similar to those seen in the mononuclear complex, and others were seen in the NMR spectrum of $[Os(NH_3)_5(TFMS)](TFMS)_2$, one of the starting reagents. The more intense ones have a small temperature dependence and are presumably impurities that interact weakly with one or more of the paramagnetic entities in the solution. The peak at 11.0 ppm is broader and has a temperature dependence that makes it a possibility for a dtdp proton, but it did not change intensity in an earlier

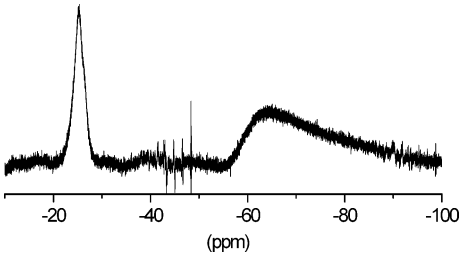

Figure 4. ^{1}H NMR of the ion complex $[(NH_3)_5Os(dtdp)Os(NH_3)_5]^{6+}$ in *d*-acetone in upfield region. The spectrum is from the sample purified by cation-exchange chromatography.

sample where the 114 ppm peak decayed away due to some reaction. Thus we deduce that the only peaks that can be attributed to the binuclear complex are the three or four peaks in Figure 4 with very paramagnetic shifts between −25 and −65 ppm. We initially expected to find only two peaks for dtdp in $[(NH_3)_5Os(dtdp)Os(NH_3)_5](TFMS)_6$ due to free rotation of the pyridine rings, but the asymmetry of the broad peak around −65 ppm suggests that it is several peaks, and there is a small broad peak about −39 ppm that is more prominent in some preparations.

The presence of at least three forms for the $[(NH_3)_5Os(dtdp)Os(NH_3)_5]^{6+}$ ion as shown by the NMR peaks of ammonia in the downfield region, shifts greater than 10 ppm, can best be explained as geometric isomers, and the reasoning is presented below after the EPR spectra are discussed. This will also explain the presence of more than two ligand peaks in the upfield region of the NMR spectrum, shifts less than 0 ppm. The most important conclusion to be drawn from the NMR results is the order of magnitude change in the paramagnetic shift of the ligand protons when two osmium ions are attached to both ends of the ligand compared to that of only one osmium ion. This means that the presence of two osmium ions leads to a significant transfer of spin into the π system of both rings and this could only be *promoted by the disulfur bridge*. No attempt was made to separate the contact and pseudocontact shifts as was done for the mononuclear complexes due to the difficulties presented by the fact, shown by the EPR, that this binuclear complex is an $S = 1$ molecule, not two separate $S = {}^1/_2$ spins.

EPR. The EPR spectra at 77 K of powdered samples of $[Os(NH_3)_5(dtdp)](TFMS)_3$ and $[Ru(NH_3)_5(dtdp)](TFMS)_3$ complexes are shown in Figure 5. In the ruthenium complex spectrum we observed an apparent axial symmetry and the best fit of the experimental data to the powder spectrum[29] is obtained for $g_\perp = 2.29$, $g_{||} = 1.91$. For the system containing osmium, the best result has been obtained for $g_1 = 2.24$, $g_2 = 1.75$, and $g_3 = 1.67$. Although the three lines are not clearly seen in Figure 5, the lines are well resolved in the spectrum of another batch of the same sample diluted in acetone, taken at 77 K.

In these low-spin systems, the metal ions (Os or Ru) have octahedral coordination with five NH_3 and one dtdp. The interpretation of the *g* values in strong-field d^5 systems has a large confusing literature of different equations with differing sign conventions that is replete with errors. This

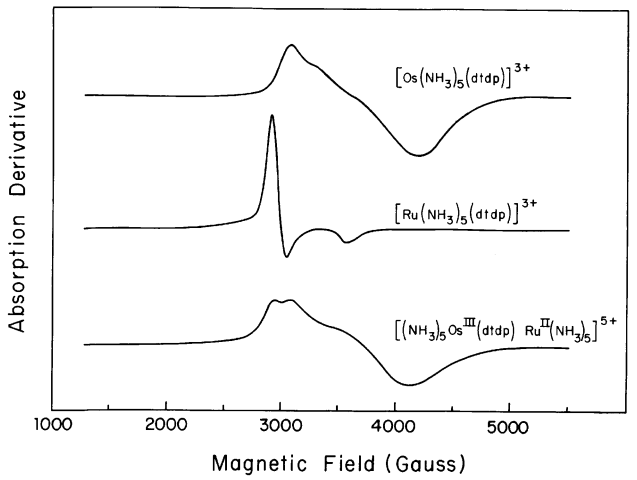

Figure 5. EPR spectra of the complexes ions: $[Os(NH_3)_5(dtdp)]^{3+}$, $[Ru(NH_3)_5(dtdp)]^{3+}$, and $[(NH_3)_5Os^{III}(dtdp)Ru^{II}(NH_3)_5]^{5+}$ in powdered sample, $T = 77$ K.

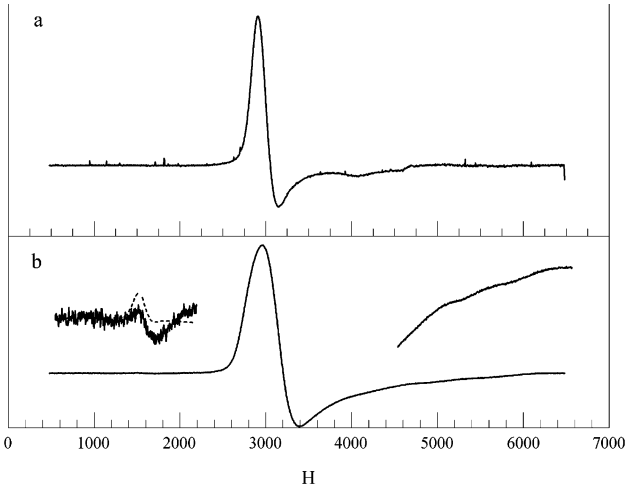

Figure 6. EPR spectrum of $[(NH_3)_5Os(dtdp)Os(NH_3)_5]^{6+}$. (a) In acetone at 77 K, $\nu = 9.45$ GHz. (b) In solid. Inset on left in b shows half-field transition. The dashed line is from a simulation using parameters given in paper. Inset on right in b shows "double bumps" in region of 5000−6000 G.

has been reviewed by one of the authors (B.R.M.),[30,31] who proposed a system where the *z* axis is taken to be the direction associated with the largest distortion in energy for the three t_2 orbitals. In this analysis the equations for the three principal *g* values are given in terms of four parameters: Δ, the difference in energy between d_{xy} and the average energy of d_{xz} and d_{yz}; *V*, the difference in energy between d_{xz} and d_{yz}; *k*, the orbital reduction factor; and λ, the spin−orbit parameter. Since the equations use only the ratios Δ/λ and V/λ, there are only three parameters to be obtained from three *g* values. Using the equations of McGarvey[30] and a value of $\lambda = 1000$ cm^{-1} for Ru^{3+}, we obtain $\Delta = 133$ cm^{-1}, $k = 1.13$. Taking $\lambda = 2760$ cm^{-1} for Os^{3+}, we obtain $\Delta = -597$ cm^{-1}, $V = -77$ cm^{-1}, $k = 0.92$. It has been shown[29] that Δ is a measure of the π interaction between the t_2 orbitals and the ligand orbitals and, if there is only one orbital that has a π interaction with the ligand, there will be axial symmetry in the **g** tensor and the parallel axis will be perpendicular to the t_2 orbital with which π interacts. This means that, for the molecules considered here, the parallel axis will be perpendicular to the M−N bond and in the plane of the dtdp ligand. Thus axial symmetry in *g* does not mean axial symmetry in the complex, as many researchers have mistakenly believed. A positive Δ means the metal is acting as a π acceptor to the ligand, and a negative value means a π donor. Thus $[Ru^{III}(NH_3)_5]$ is a π acceptor to dtdp (Δ is much larger in magnitude for other ligands)[32] and $[Os^{III}(NH_3)_5]$ is acting as π donor to dtdp.

The nonzero value for *V* in the case of $[Os^{III}(NH_3)_5(dtdp)](TFMS)_3$ requires an explanation as it has not been seen in other $[(Ru,Os)(NH_3)_5L]^{3+}$ systems. The negative value of Δ means that d_{xy} is lower in energy than d_{xz},d_{yz}. Thus placing five electrons into these energy levels produces a degenerate ground state. The Jahn−Teller theorem tells us that such a system must distort to give three different *g* values. This effect has been seen[31] in the tetragonal $t\text{-}RuCl_4L_2$ and $t\text{-}RuL_4Cl_2$ complexes where the sign reversal in Δ takes place.

The EPR spectrum of the binuclear complex $[(NH_3)_5Os(dtdp)Fe(CN)_5](TFMS)_3$ with 2.25($g_{\|}$) and 1.69 ($g_{\perp}$). Thus the presence of $[Fe^{II}(CN)_5]$ attached to the other end of the dtdp has no effect on the Os(III) end. The same cannot be said for the binuclear complex $[(NH_3)_5Os^{III}(dtdp)Ru^{II}(NH_3)_5](TFMS)_3(PF_6)_2$ (see Figure 5). The signal appears to be a mixture, but the bulk of the signal is similar to the signal of $[Os(NH_3)_5(dtdp)](TFMS)_3$ except that $g_{\|}$ is considerably smaller and *V* is larger. The extra signal could be from a Ru(III) impurity or from the binuclear species with Os(II)−Ru(III). It is clear, however, that the Ru(II) has a pronounced effect on the Os(III) signal.

The EPR spectra of the $[(NH_3)_5Os(dtdp)Os(NH_3)_5]^{6+}$ ion complex in the solid state and in the frozen liquid state are shown in Figure 6. The liquid was the same solution somewhat diluted that was used in the NMR spectrometer, and the spectra were taken within a couple of hours of the NMR spectra. The spectra have a similar shape but are different. The double bump at higher fields is present in both, but it occurs in the 5000−6000 G region in the solid compound while in the frozen liquid it occurs in the 4000−5000 G region. The high signal-to-noise of the solid signal makes it possible to detect the half-field forbidden transition at 1500 G, which is a signature for an $S = 1$ system. As will be seen from the discussion below, we are certain that the transition is also present in the frozen liquid system but below the signal-to-noise ratio of the spectrum. Because we suspected the water contamination in earlier NMR samples to contribute to the changes found in the NMR spectra, we added some water to the solution sample and redid the EPR spectrum several days later. Indeed some changes were observed, the most prominent being the appearance of a *S*

(30) McGarvey, B. R. *Quím. Nova* **1998**, *21*, 206
(31) McGarvey, B. R. *Coord. Chem. Rev.* **1998**, *107*, 75−92.
(32) Magnuson, R. H.; Lay, P. L.; Taube, H. *J. Am. Chem. Soc.* **1983**, *105*, 2507−2509.
(33) Shi, C.; Anson, F. C. *Inorg. Chem.* **1997**, *36* (12), 2682−2687.

= 1 half-field signal above the signal-to-noise and a widening of the splitting of the two bumps by about 50 G.

The double bumps might be explained as a mixture of two spin $^1/_2$ species with different $g_{||}$ values, but we think it arises from the spin−spin zero field interaction in an $S = 1$ system and have tried to simulate it as such. Such a simulation is shown for the frozen liquid spectrum in Figure 6. The three energy levels of an $S = 1$ system are obtained from the spin-Hamiltonian:

$$H = \beta_e(g_x S_x H_x + g_y S_y H_y + g_z S_z H_z) + D\left(S_z^2 - \frac{2}{3}\right) + E(S_x^2 - S_y^2) \quad (1)$$

where D and E are the anisotropic components of the spin−spin interaction. By convention $|E| \leq |D|/3$. The program assumes the major spin−spin distortion axis to be the z axis, but we do not have to assign $g_{||}$ to the z axis. In fact, we can give any values to the three principal axes of the system. This is important because, as mentioned above, the $g_{||}$ axis is perpendicular to the metal nitrogen bond. The simulation shown in Figure 6 assumed the parallel axis of the g matrix to be z with values of $g_z = 1.61$, $g_x = g_y = 2.26$, $D = 150$ G, and $E = 25$ G. However, it turns out that an equally good fit can be obtained by using $g_x = 1.59$, $g_z = g_y = 2.27$, $D = 150$ G, and $E = -50$ G. It is to be noted that both simulations give similar values for D, which depends mainly on the separation of the two bumps. When we attempted to simulate the solid-state spectrum, we found that, if we fitted the two bumps and the $g_\perp$ region, we also fitted the position and intensity of the half-field peak but the region between 4000 and 5000 was not well simulated. The parameters used in the simulation were $g_x = 1.30$, $g_z = g_y = 2.19$, $D = 200$ G, and $E = -66$ G. Again a similar spectrum could be made for $g_z = 1.30$ etc. A somewhat better simulation results from adding the frozen liquid simulation to this simulation in the proportion of 40:60. We suggest that the solid spectrum consists of a mixture of conformations with different $g_{||}$ values and D values ranging from 150 to 200 G. The conformations in solution then favor the lower values of D and $g_{||}$ or different conformations have different solubilities. Incidentally, our simulations tell us that going from a D of 150 G to 200 G increases the intensity of the half-field transition above the signal-to-noise of the frozen liquid spectrum.

The EPR of both the frozen solution and the starting solid does not show any large signal from $S = ^1/_2$ systems similar to that given by $[Os(NH_3)_5(dtdp)](TFMS)_3$, whose spectrum is known.[6] Since we will propose below that such an $S = ^1/_2$ system is present to the extent of 10−15% in the liquid solutions, it is necessary to explain why the EPR spectrum of an $S = ^1/_2$ system is not evident in the EPR spectrum of a frozen solution. The detection of small amounts of $S = ^1/_2$ species in the presence of a much larger $S = 1$ species is difficult because the intensity of a triplet state ($S = 1$) EPR spectrum is four times that of a doublet state ($S = ^1/_2$) with the same g value and concentration. This comes about because, one, there are two transition peaks in the EPR spectrum of $S = 1$ spin systems and, two, the intrinsic intensity of each peak is double that of an $S = ^1/_2$ spin system.

Finally it must be noted that the positions of $g_{||}$ and $g_\perp$ are inverted from those of the mononuclear complex of osmium. The g values for the frozen liquid give a $\Delta = +650$ cm^{-1}. For the solid, $\Delta = +900$ cm^{-1}. Thus both osmiums have a different ground state in the binuclear complex than they have in the mononuclear complex. This coupled with the $S = 1$ state and the NMR evidence leads to the conclusion that the disulfide bridge allows for a large electron delocalization over the dtdp ligand.

Cyclic Voltammetry. The cyclic voltammetry curves are reversible over a wide range of hydrogen ion concentrations (10^{-6}−10^{-3} M) for the Os(III)/Os(II) couple in the title complex.[33] The cyclic voltammogram of $[Os(NH_3)_5(dtdp)]^{3+}$ in aqueous solutions, $C_{H+} = 1.0 \times 10^{-5}$ M, exhibits only a one-electron reversible electrochemical process with $E_{1/2} = -0.69 \pm 0.07$ V versus SCE. Since the $E_{1/2}$ for the redox couple Os(III)/Os(II) in $[Os(NH_3)_5H_2O]^{3+}$ is reported to be −0.97 V (versus SCE), the substitution of the water ligand by dtdp in the osmium center stabilizes the Os(II) with respect to the oxidation by 0.29 V. This stabilization in terms of free energy is similar within the limits of the experimental error (±10 mV) to the same observed for the $[Ru(NH_3)_5(dtdp)]^{3+/2+}$ system (0.29 V), but higher than that observed for $[Fe(CN)_5(dtdp)]^{2-/3-}$ and $[Ru(CN)_5(dtdp)]^{2-/3-}$ systems, with $E^{\circ\prime}_{M(III)/M(II)}$ of these corresponding aquo species: 0.11 and 0.01 V, respectively.[5,6]

As judged from the $E_{1/2}$ values, the extension of the back-bonding Os(II)→L, for L = py, 4,4′-bipy, and dtdp,[5−8] increases as follows: py < dtdp < 4,4′-bipy. The same order was observed for the iron and the ruthenium species.[5,7a,8]

The determination of the pK_a value of the protonated dtdp ligand coordinated to the metal centers ($Fe^{II,III}$, $Ru^{II,III}$, $Os^{II,III}$), can be used to estimate the back-bonding capability of these metal centers.[14] As judged from the radial extension and energy of the d metal orbitals, Os^{II} is expected to exhibit a higher pK_a value, since the 5d orbitals are higher in energy than the 4d (Ru) or 3d (Fe) orbitals and therefore closer in energy to that of the ligand antibonding orbital.[14,15]

Voltammetric measurements in the aqueous solutions containing the Os−dtdp species at different hydrogen ion concentrations allow one to calculate the pK_a for the reactions

$$[Os(NH_3)_5(dtdpH)]^{4+} + H_2O \rightleftharpoons [Os(NH_3)_5(dtdp)]^{3+} + H_3O^+ \quad (2)$$

$$[Os(NH_3)_5(dtdpH)]^{3+} + H_2O \rightleftharpoons [Os(NH_3)_5(dtdp)]^{2+} + H_3O^+ \quad (3)$$

as equal to 3.5 ± 0.1 and 5.5 ± 0.1, respectively. The pK_a value 3.5 ± 0.1 for reaction 1, calculated from the cyclic voltammetric data, is in very good agreement with the one calculated from spectrophotometric measurements at 312 nm: 3.4 ± 0.1.

The $[Os(NH_3)_5(dtdpH)]^{3+}$ acid is weaker than the $[Ru(NH_3)_5(dtdpH)]^{3+}$ acid by 0.30 pK_a unit only (see Table 2);

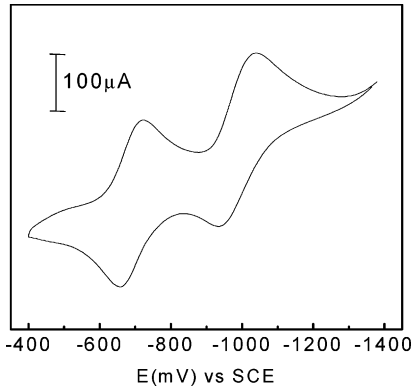

Figure 7. Cyclic voltammogram of the binuclear complex $[(NH_3)_5Os(dtdp)Os(NH_3)_5]^{6+/5+/4+}$ in NaTFA, 0.1 M, pH 3.23, $\mu = 0.1$ M, 25 °C, 50 mV/s.

Table 2. pK_a Data for Complexes of dtdp with Ruthenium and Osmium and for the Free Ligand

species	pK_a
$(dtdpH)^{+}$ [a]	4.80
$(dtdpH_2)^{2+}$ [a]	2.70
$[Os(NH_3)_5(dtdpH)]^{3+}$	5.50
$[Os(NH_3)_5(dtdpH)]^{4+}$	3.50[b]
$[Ru(NH_3)_5(dtdpH)]^{3+}$	5.20
$[Ru(NH_3)_5(dtdpH)]^{4+}$	3.20

[a] Reference 26. [b] Obtained independently through spectrophotometric and voltammetric measurements.

this behavior is similar to the behavior observed for $[Os(NH_3)_5(dtdpH)]^{4+}$ and $[Ru(NH_3)_5(dtdpH)]^{4+}$ acids.

The $[Os(NH_3)_5]^{3+}$ moiety is expected to be a stronger Lewis acid than the corresponding $[Ru(NH_3)_5]^{3+}$ fragment.[7a,10] However, in this $[M(NH_3)_5(dtdpH)]^{4+}$ species the σ electronic effect has predominance over back-bonding and a decrease of 1.3 and 1.6 pK_a units with respect to the free $dtdpH^+$ acid is observed.

In the $[Os(NH_3)_5(dtdpH)]^{3+}$ species, an increase in 0.7 pK_a unit of basically the nitrogen atom of the uncoordinated pyridine ring reflects the efficiency of the −S−S− bridge to conduct electron density. Since the polarization effects of the Os(III) are greater than that of Os(II) and the extension of the back-bonding Os(III)→dtdp should be smaller than in Os(II)→dtdp, the $[Os(NH_3)_5dtdpH]^{4+}$ exhibits a pK_a value which is 1.30 units smaller than that of free $dtdpH^+$ ion.

The change in the metal−metal interaction can be also followed through the changes in ($E_{1/2}$) separation of the successive redox couples, K_c values, energy of the intervalence band, and electron paramagnetic resonance.[34]

In the voltammogram for $[(NH_3)_5Os(dtdp)Os(NH_3)_5]^{6+/5+/4+}$ two redox processes were observed, $(E_{1/2})_1 = -985$ mV and $(E_{1/2})_2 = -670$ mV vs SCE, with $\Delta E_{1/2} = 315$ mV (see Figure 7).

The comproportionation constant (K_c),

$$[Os^{II},Os^{II}] + [Os^{III},Os^{III}] \overset{K_c}{\rightleftharpoons} 2[Os^{II},Os^{III}] \qquad (4)$$

was calculated as 2.0×10^5. This K_c value for the $[Os^{II}(dtdp)Os^{III}]$ species is slightly higher than the value of 8.0×10^4 determined for the analogous ruthenium binuclear complexes[5,6] and consistent with the more extensive participation of the 5d orbitals of osmium, leading to a larger electronic coupling in this complex than in the ruthenium analogues.[5,6]

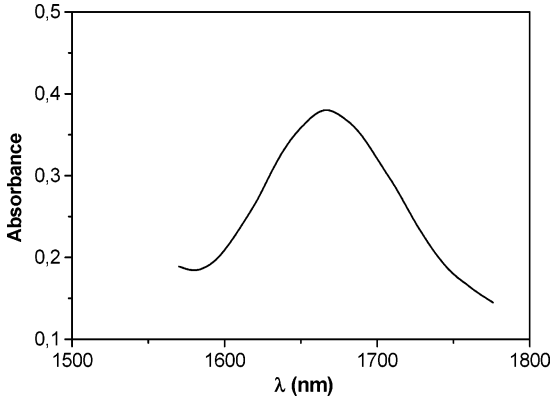

Figure 8. NIR spectrum for the mixed-valence $[(NH_3)_5Os(dtdp)Os(NH_3)_5]^{5+}$ ion; $C = 5.40 \times 10^{-5}$ M, in D_2O/DCl, 0.01 M.

Table 3. Comproportionation Constants and Near-IR Absorption Data for Binuclear Complexes of Osmium, Ruthenium, and Iron

species[a]	λ_{max} (nm)	ϵ (M^{-1} cm^{-1})	K_c	H_{AB} (cm^{-1})	$\Delta\bar{\nu}_{1/2}$	α[g]
$[(NH_3)_5Os(pz)Os(NH_3)_5]^{5+}$ [b]	2940	3000	7×10^{12}	510[f]	2800[f]	0.15
$[(NH_3)_5Ru(pz)Ru(NH_3)_5]^{5+}$ [c]	1570	5000	4×10^6	3145	1400	0.49
$[(CN)_5Fe(pz)Fe(CN)_5]^{5-}$ [d]	1200	2200	5×10^5	900	4800	0.11
$[(NH_3)_5Os(dtdp)Os(NH_3)_5]^{5+}$	1665	3500	2×10^5	780	3700	0.13
$[(NH_3)_5Ru(dtdp)Ru(NH_3)_5]^{5+}$ [e]	1500	4260	8×10^4	855	4300	0.12
$[(CN)_5Fe(dtdp)Fe(CN)_5]^{5-}$ [e]	1195	900	1×10^2	466	4020	0.06

[a] pz = pyrazine, dtdp = 4,4′-dithiodipyridine. [b] Reference 35. [c] Reference 36. [d] Reference 38. [e] References 5 and 6. [f] Calculated from the spectrum of ref 36. [g] Describe the electronic delocalization in ground state, if $\alpha \approx 0$ (class I), $0 < \alpha < \sqrt{2}/2$ (class II), $\alpha = \sqrt{2}/2$ (class III).[2]

The characteristics of the MMCT band for the $[(NH_3)_5Os(dtdp)Os(NH_3)_5]^{5+}$ ion complex are 1665 nm, $\epsilon = 3.5 \times 10^3$ M^{-1} cm^{-1}, bandwidth at half-intensity, $\Delta\bar{\nu}_{1/2} = 3.7 \times 10^3$ cm^{-1}; $\alpha = 0.13$ and electronic coupling, $H_{AB} = 7.8 \times 10^2$ cm^{-1} (see Figure 8). These values when compared with the values for the mixed-valence complexes of ruthenium and iron with the dtdp and pyrazine ligands also suggest a strong coupling between the two osmium centers (see Table 3).

Similarly, the cyclic voltammogram for $[(NH_3)_5Os(dtdp)Fe(CN)_5]^{+1/0/-1}$ systems indicate the presence of two redox processes, $(E_{1/2})_1 = -726$ mV and $(E_{1/2})_2 = 280$ mV. The differences observed between the $E_{1/2}$ values of this unsymmetrical binuclear complex and the $E_{1/2}$ values of the respective monomers ($E_{1/2} = -690$ mV and $E_{1/2} = 255$ mV for $[Os(NH_3)_5(dtdp)]^{3+/2+}$ and $[Fe(CN)_5(dtdp)]^{-2/-3}$, respectively) are close, suggesting that the metal centers in the binuclear species are interacting weakly.[37,39,40]

(34) Yeomans, B. D.; Humphrey, D. G.; Heath, G. A. *J. Chem. Soc., Dalton Trans.* **1997**, 4153−4166.
(35) Lay, P. A.; Magnuson, R. H.; Taube, H. *Inorg. Chem.* **1988**, *27*, 2364−2371.
(36) Creutz, C.; Taube, H. *J. Am. Chem. Soc.* **1973**, *95*, 1086−1094.
(37) Moreira, I. S.; Lima, E. C.; Franco, D. W. *Inorg. Chim. Acta* **1998**, *267*, 93−99.
(38) Felix, F.; Ludi, A. *Inorg. Chem.* **1978**, *17*, 1782−1783.
(39) Henderson, W. W.; Shepherd, R. E. *Inorg. Chem.* **1985**, *24*, 2398−2404.
(40) Creutz, C. *Prog. Inorg. Chem.* **1983**, *30*, 1−71.

The voltammogram for $[(NH_3)_5Os^{III}(dtdp)Ru^{II}(NH_3)_5]^{5+}$ species exhibits two well-defined reversible one electron processes $(E_{1/2})_1 = -710$ mV and $(E_{1/2})_2 = -140$ mV vs SCE. The electrochemical process with $(E_{1/2})_1 = -710$ mV occurs within the limits of the experimental error, at the same potential of the $[Os(NH_3)_5(dtdp)]^{3+/2+}$ process, and therefore has been assigned to the Os(III)/Os(II) couple in the binuclear species. This would be interpreted as a characteristic of a weakly coupled class II dimer in a solvent of high dielectric constant.[40] Nevertheless, the fact that the $Os^{III}-Ru^{III}/Os^{III}-Ru^{II}$ potential is 60 mV more positive than that observed in the ruthenium monomer complex would suggest the accumulation of charge on the metal centers, reflecting the stabilization of Ru(II)−dtdp by binding to Os(III).

For comparison proposes, an estimate of the H_{AB} values has been carried out assuming the maximum internuclear distance as equal to 7.8 ± 0.5 Å, from available crystallographic data for the free ligand[41] and using eq 5.[42] The

$$H_{AB} = \frac{2059 \times 10^{-2}}{r}(\epsilon_{max}\,\bar{\nu}_{max}\Delta\bar{\nu}_{1/2})^{1/2}(cm^{-1}) \qquad (5)$$

intervalence bands for unsymmetrical complexes have the following characteristics: $[(NH_3)_5Os^{III}(dtdp)Ru^{II}(NH_3)_5]^{5+}$, $\lambda_{max} = 965$ nm, $\epsilon = 2.2 \times 10^2$ M^{-1} cm^{-1}, $\Delta\bar{\nu}_{1/2} = 3.3 \times 10^3$ cm^{-1}, and $H_{AB} = 2.2 \times 10^2$ cm^{-1}; $[(NH_3)_5Os^{III}(dtdp)Fe^{II}(CN)_5]$, $\lambda_{max} = 790$ nm, $\epsilon = 7.5 \times 10$ M^{-1} cm^{-1}, $\Delta\bar{\nu}_{1/2} = 5.4 \times 10^3$ cm^{-1}, and $H_{AB} = 2.0 \times 10^2$ cm^{-1}.

This behavior is similar to the behavior reported by Henderson and Shepherd,[39] who pointed out that the unsymmetrical complexes, compared to the symmetrical complexes, exhibit lower H_{AB} values.

For the $[(NH_3)_5Os^{III}(dtdp)Fe^{II}(CN)_5]$ complex, the presence of the cyanide ligands, a good π-acceptor, would reduce the Fe(II) d_π electron density to back-bonding interaction. Therefore, as indicative of the low interaction between the osmium and the iron center, the intervalence band is observed at 790 nm, whereas for the $[(NH_3)_5Os^{III}(dtdp)Ru^{II}(NH_3)_5]^{5+}$ dimer, where no π-acceptor ligands are present in the coordination sphere, the IT band is at 965 nm.

Isomers of $[(NH_3)_5Os(dtdp)Os(NH_3)_5]^{6+}$ Ion. The NMR tells us that there are three different isomer forms of the $[(NH_3)_5Os(dtdp)Os(NH_3)_5]^{6+}$ complex ion in solution. We propose that this can be explained by assuming that there is double-bond character in the −S−S− bond, making cis−trans isomers possible. We further propose that the extent of delocalization of spin required to explain the existence of the triplet ground state plus the extensive delocalization of spin in the π system of the aromatic rings can only be explained by assuming that the trans isomer has both pyridine rings and the −S−S− bond in the same plane to facilitate formation of a π MO over the whole dpdt ligand. This rigidity in the trans isomer would also explain the existence of more than two NMR peaks in the −25 to −65 ppm region of the NMR spectrum because the lack of rotation about the py−S bond would make the (3,5) and (2,6) protons inequivalent. This trans isomer would then be the main species that we see in the NMR spectrum of the $[(NH_3)_5Os(dtdp)Os(NH_3)_5]^{6+}$ ion complex and would be the species that gives rise to the $S = 1$ EPR spectrum observed. The ammonia peaks at 151 and 90 ppm belonging to the second most abundant form can then be assigned to the cis isomer. Since the cis isomer cannot form a π MO between the pyridine rings and the S−S bridge, the two $S = {}^1/_2$ units would be disconnected and give EPR and NMR spectra similar to those of $[Os(NH_3)_5(dtdp)](TFMS)_3$. We have no proposed structure for the third form present in low concentration that was observed in the NMR spectrum. The difference in the EPR spectra of the binuclear complex between the frozen solution and solid samples can be readily explained in terms of small distortions in the planarity of the trans isomer in the two states, which would cause significant changes in the g and D parameters.

Conclusions

All together, the results emphasize the importance of the −S−S− bridge as an electron conductor in mono- and binuclear complexes. By far the most striking evidence as found by EPR and NMR is in the binuclear complex $[(NH_3)_5Os(dtdp)Os(NH_3)_5](TFMS)_6$ which is in a triplet state with large delocalization of unpaired spin in the two pyridine rings. Until now we have not mentioned the singlet state of the binuclear complex, which has to be present in the solid and the solution at a population about a third that of the triplet state. Some of the unidentified diamagnetic peaks in the NMR could come from it, but more likely the peaks we are seeing are a time average of the peaks for the two systems.

Preliminary experiments in the *trans*-$[(NH_3)_5Ru(dtdp)Ru(NH_3)_4(dtdp)Ru(NH_3)_5]^{6+}$ trinuclear complex, prepared by reacting $[Ru(NH_3)_5(dtdp)](PF_6)_2$ and $[Ru(NH_3)_5(H_2O)](PF_6)_2$ complexes in 1:2 stoichiometric ratio, have been started.

Acknowledgment. We are thankful to the Brazilian agencies FAPESP, CNPq, and CAPES for financial support and to Prof. Heloise Pastore for reading the first version of the English manuscript. The authors are also indebted to Profs. S. S. Isied and R. E. Shepherd for the discussions and suggestions.

IC034630O

(41) (a) Raghavan, N. V.; Seff, K. *Acta Crystallogr.* **1977**, *B33*, 386−391. (b) Lee, J. D.; Bryant, M. W. R. *Acta Crystallogr.* **1969**, *B25*, 2094−2101.

(42) Robin, M. B.; Day, P. *Adv. Inorg. Radiochem.* **1967**, *10*, 247−422.